



HAL
open science

LES of Turbulent Forced Convection of a Non-Newtonian Fluid in a Stationary Pipe: The Mean Quantities

Mohamed Abdi, Meryem Ould-Rouiss, Abdelkader Noureddine

► **To cite this version:**

Mohamed Abdi, Meryem Ould-Rouiss, Abdelkader Noureddine. LES of Turbulent Forced Convection of a Non-Newtonian Fluid in a Stationary Pipe: The Mean Quantities. 1 ère Conférences Sur Les Energies Renouvelables & Les Matériaux Avancés ERMA'19, Dec 2019, Relizane, Algeria. hal-04075307

HAL Id: hal-04075307

<https://hal.science/hal-04075307v1>

Submitted on 20 Apr 2023

HAL is a multi-disciplinary open access archive for the deposit and dissemination of scientific research documents, whether they are published or not. The documents may come from teaching and research institutions in France or abroad, or from public or private research centers.

L'archive ouverte pluridisciplinaire **HAL**, est destinée au dépôt et à la diffusion de documents scientifiques de niveau recherche, publiés ou non, émanant des établissements d'enseignement et de recherche français ou étrangers, des laboratoires publics ou privés.

LES of Turbulent Forced Convection of a Non-Newtonian Fluid in a Stationary Pipe: The Mean Quantities

Mohamed Abdi^{1, a}, Meryem Ould-Rouiss², Abdelkader Noureddine¹

¹ Université USTO Mohamed Boudiaf, Laboratoire de Mécanique Appliquée, BP 1505 Oran EL M'Naouar Oran, Algeria

² Université Paris-Est, Laboratoire de Modélisation et Simulation Multi Echelle, MSME, Paris-Est, UMR 8208 CNRS, 5 bd Descartes, 77454 Marne-la-Vallée, Paris, France

Abstract. A fully developed forced convection heat transfer of a thermally independent shear thinning ($n=0.75$) and Newtonian fluids flowing inside a uniform heated axially pipe has been carried out numerically by means of the large eddy simulation (LES) with an extended Smagorinsky model at a simulation's Reynolds and Prandtl numbers equal to $Re_s=4000$ and $Pr_s=1$ respectively. The present investigation aims to ascertain the accuracy and reliability of the LES laboratory code predicted results and evaluate the effectiveness of the extended Smagorinsky model to resolve and describe the evolution of the main mean flow quantities and thermal statistics in the present computational domain especially at the wall vicinity. The Computations are based on a finite difference scheme, second order accurate in space and in time, the numeric resolution is 65^3 grid points in r , θ and z direction respectively, with length of the domain of $20R$. The predicted results show an excellent agreement with the DNS results, the main findings show that the present LES laboratory code can be considered as a powerful tool for predicting the mean thermal quantities of the Non-Newtonian fluid. The reduction in the fluid flow index (n) results in enhancement in the mean axial velocity and a pronounced attenuation in the mean temperature over the radial direction, where leads also to noticeable drop in the average Nusselt number.

1 Introduction

The turbulent forced convection heat transfer of the Non-Newtonian fluids is of practical importance in many industrial applications for example in paper making, drilling of petroleum products, slurry transportation and processing of food and polymer solutions. a considerable amount of literature has been carried out on the flow of the Newtonian fluid in a straight pipe, where is contains a number of well-documented, either experimentally or numerically by [1] [2] [3] [4] [5].

On the other hand, the turbulent Non-Newtonian fluid in axially pipe has been largely investigated experimentally and numerically over the recent decades, among them [6] [7] [8] [9] [10] [11] [12] [13].

Despite the particular importance of the heat transfer of the Non-Newtonian fluids in the above-mentioned engineering application, there is a paucity of scientific literature focusing specifically on the forced convection heat transfer of Non-Newtonian fluids in such issue. Toward this end, the present study seeks to ascertain the accuracy and reliability of the LES laboratory code predicted results and evaluate the accuracy of the employed extended Smagorinsky model to predict the effect of shear thinning flow index on the main thermal statistics, in addition to shed further light on shear thinning rheological and thermal behaviour in the turbulent flow. Toward this end, a LES with an extended Smagorinsky model has been applied to investigate numerically the fully developed turbulent forced convection heat transfer of a shear thinning ($n=0.75$) and Newtonian fluids in a uniform heated axially stationary pipe at a simulation's Reynolds and Prandtl numbers of $Re_s=4000$ and $Pr_s=1$ respectively, with an adequate grid resolution of 65^3 grid points in r , θ and z direction respectively and a domain length of $20R$. The present paper is organized as: governing equations and numerical procedure are presented in section 2. the mean flow and

thermal quantities are presented in section 3 and finally section 4 summarizes the results of this work and draws conclusions.

2 Governing equations and numerical procedure

2.1 Governing equations

The present study deals with a fully developed turbulent forced convection of a thermally independent shear thinning ($n=0.75$) and Newtonian ($n=1$) fluids across a heated pipe with a uniform constant heat flux q_w imposed at the pipe wall, by mean of the LES approach with an extended Smagorinsky (Fig.1), with domain length of $20R$ at the at a simulation's Reynolds and Prandtl numbers of $Re_s=4000$ and $Pr_s=1$ respectively.

The filtered equations can be expressed as follows:

$$\frac{\partial \bar{u}_i}{\partial x_i} = 0 \quad (1)$$

$$\frac{\partial \bar{u}_j}{\partial t} + \frac{\partial \bar{u}_i \bar{u}_j}{\partial x_i} = -\frac{d\bar{P}}{dx_j} + \frac{1}{Re_s} \frac{\partial}{\partial x_i} \left[\bar{\gamma}^{n-1} \left(\frac{\partial \bar{u}_j}{\partial x_i} + \frac{\partial \bar{u}_i}{\partial x_j} \right) \right] + \frac{\partial \bar{\tau}_{ij}}{\partial x_i} \quad (2)$$

$$\frac{\partial \bar{\Theta}}{\partial t} + \frac{\partial}{\partial x_j} (\bar{u}_j \bar{\Theta} - T_{\Theta j}) - \bar{u}_z \frac{d}{dz} \langle T_w \rangle = \frac{1}{Re_s Pr_s} \frac{\partial^2 \bar{\Theta}}{\partial x_k \partial x_k} \quad (3)$$

The overbar symbol ($\bar{\quad}$) denotes the filtering operation, Re_s , Pr_s are the Reynolds number and Prandtl number of the simulation and are defined respectively by: $Re_s = \rho U_{CL} R / \mu$, $Pr_s = \mu / \alpha \rho U_{CL}$.

^a Auteur principal : abdi.mohamed1@live.fr

The dimensionless temperature is defined as:

$$\Theta = \left(\langle T_w(z) \rangle - T(\theta, r, z, t) \right) / T_{ref} \quad (4)$$

T_{ref} presents the reference temperature and is defined as $T_{ref} = q_w / \rho C_p U_{CL}$, where T_w is the pipe wall temperature and $\langle \rangle$ is an average in time and periodic directions.

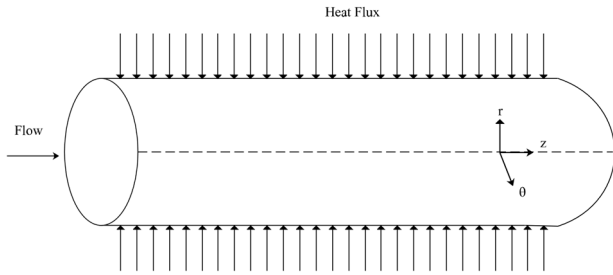


Figure 1 computational domain

2.2 Numerical procedure

The governing equations were discretized on a staggered mesh in cylindrical coordinates with a computational length in the axial direction $20R$. The numerical integration was performed by using a finite difference scheme, second-order accurate in space and in time. The time-advancement employs a fractional-step method. A third-order Runge-Kutta explicit scheme and a Crank-Nicholson implicit scheme were used to evaluate the convective and diffusive terms, respectively. The above mathematical model was implemented in a finite difference laboratory code. The grid 65^3 grid points in axial, radial and circumferential directions respectively, was found to provide an accurate prediction of the turbulence statistics, in agreement with the available data of the literature, and to give a good compromise between the required CPU-time and accuracy.

A periodic boundary condition has been applied to the axial and circumferential directions, and a usual no-slip boundary condition on the pipe wall, in addition to a uniform heat flux was imposed on the pipe wall as a thermal boundary condition. As for the grid resolution of the present mesh, uniform computational grid was applied to the axial and circumferential directions, in the radial direction, non-uniform meshes specified by a hyperbolic tangent function, the various parameter settings for mesh and LES simulations are summarized in Tab.1.

Table 1. parameters of present LES simulations $Re_s=4000$

Parameters	$n=0.75$	$n=1$
Δz^+	69.89	49.75
$r \Delta \theta^+$	21.95	15.63
Δr^+_{min}	0.0506	0.0360

Δr^+_{max}	12.4	8.83
U_b / U_{cl}	0.5329	0.4943
U_c / U_{cl}	0.6863	0.6525
$U_\tau / U_{cl} \cdot 10^3$	0.3393	0.3593
$\dot{\gamma}_{d,w}$	6.6818	5.359
$\eta_{d,w}$	0.6334	1
Re_{cr}	2250	2099.2
Re_{MR}	4873.2	4448.9
Re_g	7135.8	4448.9
Re_τ	227.16	161.71
Y_1^+	0.0239	0.0170
$f \cdot 10^3$	9.2099	10.331
Nu	17.376	17.584

3 Results and discussion

A large eddy simulation with an extended Smagorinsky model has been applied to a fully developed turbulent forced convection heat transfer of a shear thinning ($n=0.75$) and Newtonian ($n=1$) fluids at simulation's Reynolds number and Prandtl number of 4000 and 1 respectively. In the present section we will briefly analyse and discuss the LES obtained to ascertain the accuracy and reliability of the laboratory code predicted results, in addition to know to what extent the LES with the extended Smagorinsky model be able to predict the effect of shear thinning flow index on the main flow and thermal quantities, especially the mean axial velocity and mean temperature. For the validation purpose, the predicted LES results are compared reasonably with the available results of literature: experimental and numerical data of Rudman et al. [10] of a shear thinning fluid ($n=0.75$) in a turbulent pipe flow.

The Fig.2 compares the predicted mean axial velocity profile with the experimental data obtained at generalised Reynolds number of $Re_g=7027$ and DNS data at Metzner-Reed Reynolds number of $Re_{MR}=3935$. As shown in the Fig.2, the predicted profile is in an excellent agreement with the other profiles over the entire pipe radius, where the predicted profile almost coincides with the experimental and DNS profiles in each of the viscous sublayer, buffer and logarithmic layer. It should be noted here that the little marked discrepancy may be the difference in the Reynolds number value and the numerical solution procedure.

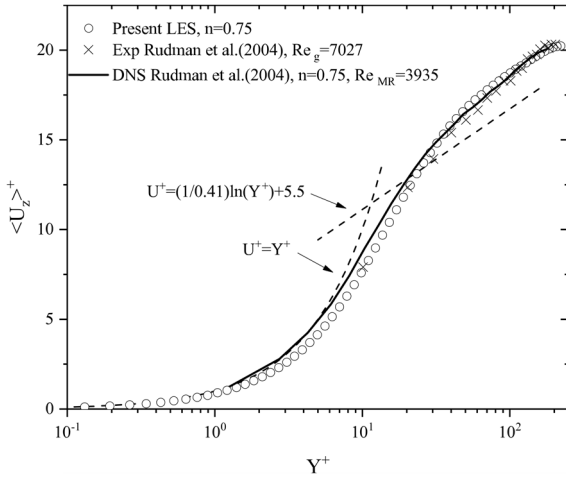


Figure 2 Validation

3.1. Mean velocity profile

In order to describe and examine the flow index influence on the streamwise velocity evolution of the shear thinning fluid along the pipe radius and comparing to that of the Newtonian one, the following paragraphs discuss the streamwise velocity revelation along the pipe radius of a shear thinning ($n=0.75$) and Newtonian ($n=1$) fluids at a simulation's Reynolds number of 4000.

The Fig.3 display the distribution of the mean velocity profile along the pipe radius, scaled by the friction velocity $U_\tau = \sqrt{\tau_w / \rho}$ against the distance from the wall in wall units Y^+ , where the dash lines represent the universal velocity distributions in the viscous sublayer and in logarithmic layer. It should be noted that the mean axial velocity is enhanced gradually with the distance from the wall Y^+ along the pipe radius in the different flow regions for the both fluids. In the viscous sublayer ($0 \leq Y^+ \leq 5$), the velocity profile coincides and agrees with the universal linear law $U^+ = Y^+$, the mean axial velocity remains constant denoting a linear velocity distribution in this region as (Fig.3). Beyond the buffer region the mean axial velocity enhances progressively further away from the wall towards the core region, where the inertia force dominants pronouncedly compared to the viscous one out of the viscous sublayer.

On the other hand, it can be seen also that the velocity profile of the shear thinning fluid coincides completely with that of the Newtonian one in the vicinity of the pipe wall, it can be said that the velocity profile are nearly independent of the rheological model, where the flow index influence is limited near the pipe wall up to approximately ($Y^+ \sim 30$). At the larger wall distance $Y^+ > 30$, the mean axial velocity profile of the Newtonian fluid in accordance with the universal logarithmic law $U^+ = 2.5 \ln Y^+ + 5.5$ in the logarithmic region ($30 \leq Y^+ \leq 200$), while the shear thinning profile lies above the universal law in this region. Beyond $Y^+ \sim 30$ the predicted profiles

deviate significantly from each other with the distance from the wall away from the wall towards the pipe centre. As shown in Fig.3 the shear thinning fluid profile is somewhat larger than that corresponding of the Newtonian one where this trend is more pronounced as closes to the core region, it is evident that this deviation in the velocity profiles is due to the difference in the fluid apparent viscosity.

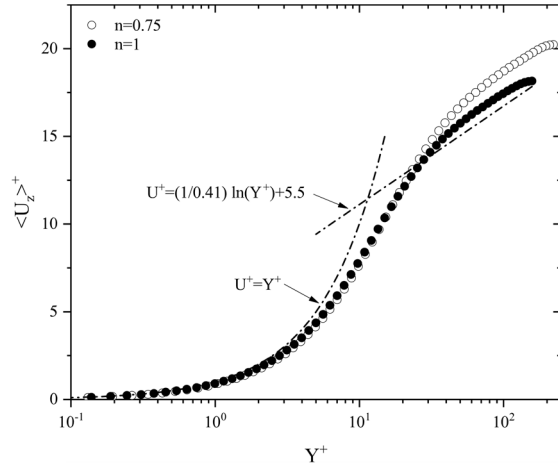


Figure 3 Mean axial velocity

In turn, the Fig.4 presents the streamwise velocity profiles along the pipe radius of the shear thinning and Newtonian fluids, in addition to the analytical velocity profile in the laminar regime for the both fluids scaled by the analytical laminar centreline velocity ($U_{CL} = (3n+1)U_b/(n+1)$), against the distance from the wall, normalized by the pipe radius (R). It can be seen from Fig.4 that the velocity profiles are characterised by a parabolic shape along the pipe regions, as mentioned above the velocity of the shear thinning ($n=0.75$) is more significant than the Newtonian one especially in the logarithmic and core region, where this is due to the difference in the fluid apparent viscosity.

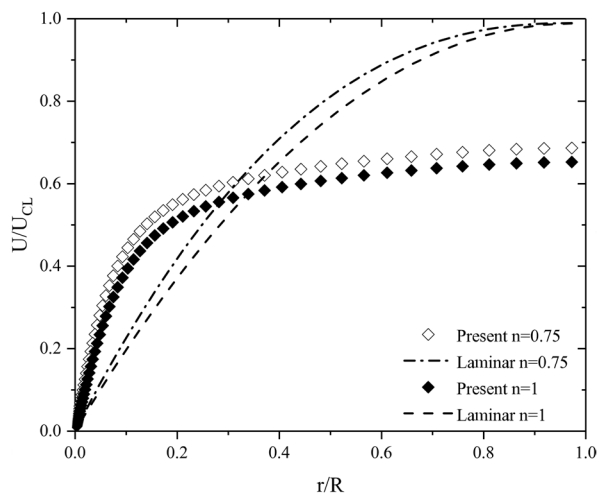


Figure 4 Mean axial velocity

3.2 Temperature profile

In order to examine the fluid flow index on the mean thermal quantities, and describe the heat transfer between the heated pipe wall and the fluids, the following paraphrases analyse and discuss the mean temperature revolution (Fig.5) and (Fig.6) in a heated pipe under a with a constant uniform heat flux q_w imposed at the pipe wall as thermal boundary condition, where the Prandtl number of the working fluid was assumed to be $Pr_s=1$.

The Fig.5 presents the shear thinning ($n=0.75$) and Newtonian ($n=1$) fluids temperature (Θ) profiles along the pipe radius (R) scaled by the reference temperature (T_{ref}), against the distance from the wall in wall units Y^+ at $Re_s=4000$, where the dash lines represent the universal temperature distributions in the conductive sublayer and in the logarithmic layer. Whereas the Fig.6 illustrates the temperature profiles scaled by the bulk temperature (Θ_b) versus the radial coordinates (r) scaled by the pipe radius (R).

It can be seen from Fig.5 that the mean temperature (Θ) is enhanced gradually further away from the wall towards the core region with the wall distance Y^+ , along the pipe radius over the different flow regions. In other words, the fluid temperature (T) attenuates progressively far away from the pipe wall, the predicted mean temperature exhibits its maximum and minimum values at the pipe wall and the pipe centreline respectively.

It can be seen also that the shear thinning and Newtonian fluids have the same trend of temperature distribution along the pipe radius, the both profiles agree and coincide with the universal linear law $\Theta^+=PrY^+$ in the vicinity of the wall ($0 \leq Y^+ \leq 1$). Beyond ($Y^+ \sim 2$) the shear thinning profile deviates significantly from the universal linear law and the profile of the Newtonian fluid, where the Newtonian profile is somewhat larger than that of the shear thinning one in the conductive sublayer ($0 \leq Y^+ \leq 5$) and in the logarithmic layer ($30 \leq Y^+ \leq 200$), this trend is more apparent as the distance from the wall is increased.

It is worth noting that the flow index affects considerably on the heat transfer between the pipe wall and the fluid flowing inside the heated pipe along the pipe radius especially out of the conductive sublayer towards the pipe centre as shown in Fig.6, where this influence is attributed to the fluid apparent viscosity.

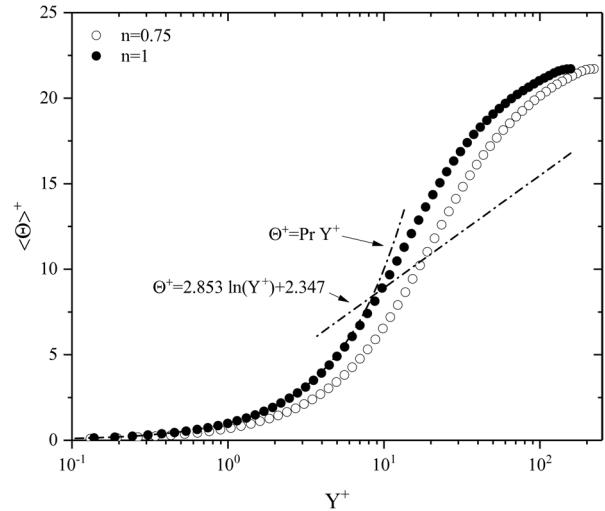


Figure 5 Mean Temperature Profile

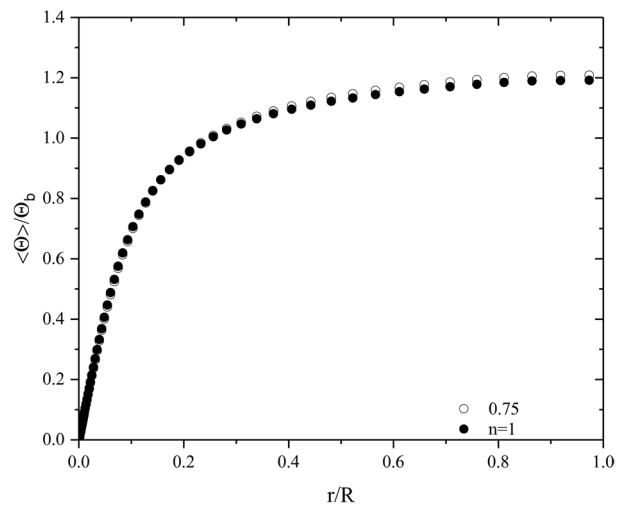
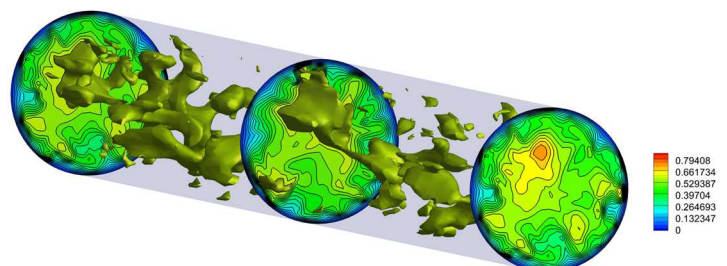


Figure 6 Mean Temperature Distribution

On the other hand, a snapshot of instantaneous mean temperature of a shear thinning fluid ($n=0.75$) in illustrated over the cross sections in Fig.7a and over longitudinal section in Fig.7b. It can be seen from these figures that smallest values of the instantaneous temperature (Θ) are located far away from the wall vicinity, while that the highest temperature values are placed near the pipe wall. It can be seen also that the small-scale structures of instantaneous mean temperature are captured in the viscous sublayer, these scales structure seems to be enlarged further away from the wall towards the core region where the large-scale structures are captured at the pipe centre, reflecting the reduction in the fluid temperature.

(a)



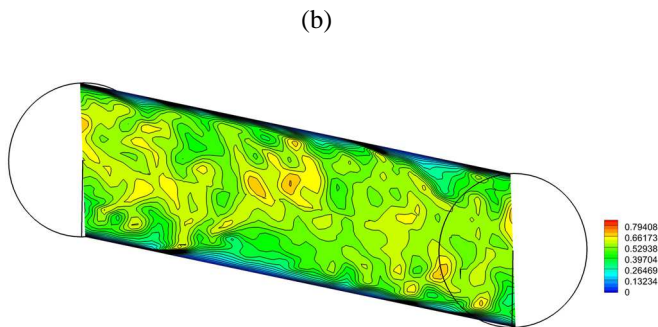


Figure 7 Instantaneous Mean Temperature

3.3 Nusselt Number

The Nusselt number is defined as $Nu = hD/k$ where $h = -k \left(\frac{\partial \bar{T}}{\partial r} \right)_w$, as mentioned in the Tab.1 the average Nusselt number enhances gradually with the fluid flow index, where the average Nusselt number of the shear thinning ($n=0.75$) fluid is found to be 17.376, and 17.584 for the Newtonian fluid. It can be said that the reduction in the fluid flow index (n) induces a pronounced attenuation in the average Nusselt number, in the other words this reduction results in a remarked attenuation in the energy transfer between the fluid and the pipe wall.

4 Conclusion

The present study reports on numerical investigation of a fully developed turbulent forced convection heat transfer of a thermally independent shear thinning ($n=0.75$) fluid flowing inside a uniform heated pipe under an uniform heat flux, by applying a large eddy simulation with extended Smagorinsky model, at simulation Reynolds and Prandtl numbers of 4000 and 1 respectively, In order to ascertain the accuracy and reliability of the LES laboratory code predicted results and evaluate the reliability of the extended Smagorinsky model to predict the main mean flow quantities and thermal statistics such as the mean streamwise velocity, mean temperature and the Nusselt number. The major conclusions of this research will be summarized:

The accuracy and reliability of the laboratory code predicted results and numerical solution procedure have been ascertained by comparing the main predicted results with those available in the literature, these findings clearly indicate that the present code can be considered as a powerful tool, where the present LES with the extended Smagorinsky model shows a great promise in predicting the thermal turbulent statistics of the turbulent forced convection heat transfer of the power law fluids in the present configuration.

On the other hand, the reduction in the fluid flow index resulted in a pronounced enhancement in the mean streamwise velocity profile along the radial coordinates especially in the logarithmic region, this deviation was raised because the difference in the fluid apparent

viscosity. In turn, this reduction in the fluid index induces a marked attenuation in the mean temperature along the pipe radius in addition to a noticeable drop in the average Nusselt number, leading to attenuate the energy transfer between the fluid and the pipe wall.

References

- [1] G. Reich and H. Beer, *Fluid flow and heat transfer in an axially rotating pipe-I. Effect of rotation on turbulent pipe flow*, Int. J. Heat Mass Transf., **vol. 32**, no. 3, pp. 551–562, Mar. (1989).
- [2] S. Satake and T. Kunugi, *Direct numerical simulation of turbulent heat transfer in an axially rotating pipe flow* Int. J. Numer. Methods Heat Fluid Flow, **vol. 12**, no. 8, pp. 958–1008, Dec. (2002).
- [3] L. Redjem-Saad, M. Ould-Rouiss, and G. Lauriat, *Direct numerical simulation of turbulent heat transfer in pipe flows: Effect of Prandtl number* Int. J. Heat Fluid Flow, **vol. 28**, no. 5, pp. 847–861, Oct. (2007).
- [4] M. Ould-Rouiss, M. Bousbai, and A. Mazouz, *Large eddy simulation of turbulent heat transfer in pipe flows with respect to Reynolds and Prandtl number effects* Acta Mech., **vol. 224**, no. 5, pp. 1133–1155, May (2013).
- [5] M. Ould-Rouiss, A. Dries, and A. Mazouz, *Numerical predictions of turbulent heat transfer for air flow in rotating pipe* Int. J. Heat Fluid Flow, **vol. 31**, no. 4, pp. 507–517, Aug. (2010).
- [6] A. B. Metzner and J. C. Reed, *Flow of non-newtonian fluids-correlation of the laminar, transition, and turbulent-flow regions* AIChE J., **vol. 1**, no. 4, pp. 434–440, Dec. (1955).
- [7] A. B. Metzner, *Non-Newtonian Fluid Flow. Relationships between Recent Pressure-Drop Correlations* Ind. Eng. Chem., **vol. 49**, no. 9, pp. 1429–1432, Sep. (1957).
- [8] D. W. Dodge and A. B. Metzner, *Turbulent flow of non-newtonian systems* AIChE J., **vol. 5**, no. 2, pp. 189–204, Jun. (1959).
- [9] F. T. Pinho and J. H. Whitelaw, *Flow of non-newtonian fluids in a pipe* J. Nonnewton. Fluid Mech., **vol. 34**, no. 2, pp. 129–144, Jan. (1990).
- [10] M. Rudman, H. M. Blackburn, L. J. W. Graham, and L. Pullum, *Turbulent pipe flow of shear-thinning fluids* J. Nonnewton. Fluid Mech., **vol. 118**, no. 1, pp. 33–48, Mar. (2004).
- [11] P. S. Gnamboe, P. Orlandi, M. Ould-Rouiss, and

X. Nicolas, *Large-Eddy simulation of turbulent pipe flow of power-law fluids* Int. J. Heat Fluid Flow, **vol. 54**, pp. 196–210, Aug. (2015).

- [12] J. Singh, M. Rudman, and H. M. Blackburn, *The influence of shear-dependent rheology on turbulent pipe flow* J. Fluid Mech., **vol. 822**, pp. 848–879, Jul. (2017).
- [13] J. Singh, M. Rudman, and H. M. Blackburn, *The effect of yield stress on pipe flow turbulence for generalised newtonian fluids*, J. Nonnewton. Fluid Mech., **vol. 249**, pp. 53–62, Nov. (2017).